and H. Tennekes, *J. Atmos. Sci.* **25**, 1015 (1968).
6. O. S. Madsen, *J. Phys. Oceanogr.* **7**, 248 (1977); J. E. Weber and A. Melsom, *ibid.* **23**, 193 (1993).
7. G. L. Mellor and T. Yamada, *Rev. Geophys.* **20**, 851 (1982).
8. See, for example, reviews by M. L. Gregg [*J. Geophys. Res.* **92**, 5249 (1987)] and E. J. Hopfinger [*ibid.*, p. 5287]. Most of the reported turbulence measurements are from the stratified thermocline below the mixed layer, but see also T. J. Shay and M. C. Gregg [*J. Phys. Oceanogr.* **16**, 1777 (1986)] for dissipation measurement in a convecting mixed layer.
9. The steady TKE equation for a high Reynolds number, horizontally homogeneous, incompressible flow [H. Tennekes and J. L. Lumley, *A First Course in Turbulence* (MIT Press, Cambridge, MA, 1972), p. 97] is typically further simplified by neglect of spatial transport terms, leading to a balance among three terms where

$$P_s + P_b = \varepsilon$$

where

$$P_s = -\left(\langle u'w'\rangle\frac{\partial U}{\partial z} + \langle v'w'\rangle\frac{\partial V}{\partial z}\right)$$

is TKE shear production

$$P_b = -\frac{g}{\rho}\langle\rho'w'\rangle = -\langle b'w'\rangle$$

is the TKE production by gravitational body forces ($\langle b'w'\rangle$ is the turbulent buoyancy flux), and

$$\varepsilon = \nu\left\langle\frac{\partial u'_j}{\partial x_i}\frac{\partial u'_j}{\partial x_i}\right\rangle$$

is TKE dissipation into heat (ν is kinematic molecular viscosity and repeated indices imply summation). In a neutrally stratified flow, buoyancy production is negligible.
10. H. Tennekes and J. L. Lumley, in (*9*), p. 98.
11. C. H. Gibson, *J. Geophys. Res.* **92**, 5383 (1987); A. Gargett, *ibid.* **95**, 15971 (1990); J. N. Moum, *J. Phys. Oceanogr.* **20**, 1980 (1990).
12. T. M. Dillon, *J. Geophys. Res.* **87**, 9601 (1982).
13. From the simplified TKE equation with no buoyancy flux, assuming that mean shear and stress are aligned in the x direction, $-\langle u'w'\rangle\partial U/\partial z = u_*^3/\lambda = \varepsilon$.
14. M. G. McPhee, *J. Geophys. Res.* **97**, 5365 (1992).
15. If m is the slope of a linear regression of y against x (temperature against depth) for five instrument clusters, m is significantly different from zero at the 95% confidence level provided

$$\left|\frac{m}{s_{y|x}\sqrt{1/\sum_{i=1}^{5}(x_i - \bar{x})^2}}\right| \geq t_{0.025|3}$$

where $s_{y|x}$ is an estimate of variability about the line, and $t_{0.025|3}$ is the 2.5 percentage point of Student's t distribution for three degrees of freedom, assuming the temperature samples are drawn from a population with independent, normally distributed errors with common variance [A. H. Bowker and G. J. Lieberman, *Engineering Statistics* (Prentice-Hall, Englewood Cliffs, NJ, 1959), p. 255]. Of 61 hourly samples in the period 86.5 to 89.0, 32 temperature gradients were statistically significant. In the subsequent regression of measured heat flux against temperature gradient, similar analysis leads to a 95% confidence interval for the regression slope (K_h) of 0.014 to 0.022. The correlation coefficient is 0.85.
16. S. Ackley, personal communication.
17. A measure of the effect of surface buoyancy flux is the Obukhov length $L = u_{*o}^3/(\kappa\langle w'b'\rangle_o)$. When the magnitude of L is comparable to, or less than, other turbulent length scales in the flow, buoyancy is dynamically important. This early in the season, most of the heat conducted to the atmosphere from the ice comes from cooling and freezing within the ice column, hence, there is little conduction near the bottom (*16*), and upward oceanic heat flux causes melting at the ice-ocean interface. Melting associated with a heat flux of 20 W m^{-2} is roughly 6 mm per day, and fresh water released by such melting would produce a stabilizing surface buoyancy flux of about $\langle w'b'\rangle_o = 1.3 \times 10^{-8}$ m^{-2} s^{-3} (*14*). With a mean value of 0.012 m s^{-1} for u_{*o}, the Obukhov length is about 300 m, far too large to be dynamically important. Even if there were a linear temperature gradient in the ice, so that freezing would produce destabilizing buoyancy flux, its magnitude would be insignificant under thick ice surrounding the instrument mast.
18. K. Hunkins, *Deep-Sea Res.* **13**, 607 (1966).
19. M. G. McPhee, in *Polar Oceanography*, W. Smith, Ed. (Academic Press, San Diego, CA, 1990), vol. 1, chap. 6.
20. V. W. Ekman, *Ark. Mat. Astron. Fys.* **2**, 1 (1905).
21. M. G. McPhee, *Boundary-Layer Meteorol.* **21**, 325 (1981). The model expresses nondimensional turbulent stress as a complex exponential $\hat{T} = e^{\delta\zeta}$, where $\hat{\tau} = \hat{\tau}/(u_{*o}\hat{u}_{*o})$; $\hat{\tau}$ is the horizontal, kinematic stress vector; $\delta = (1 - i)/\sqrt{2K_*}$ is a complex attenuation constant; and $\zeta = |f_{cor}|z/(u_{*o}\eta_*)$ is the nondimensional vertical coordinate. In the theory, K_*, the nondimensional eddy viscosity, is a constant with numerical value about 0.02, and η_* is a stability factor, equal to one if the flow is neutrally stable.
22. J. O. Hinze, *Turbulence* (McGraw-Hill, New York, ed. 2, 1975), chap. 3. In a turbulent shear flow that is anisotropic at large scales, it is often possible to identify a wave-number band at smaller scales where turbulence is nearly homogeneous and isotropic and TKE is neither produced nor dissipated. In the so-called inertial subrange, a simple power law describes the spectrum

$$S_{ww} = \frac{4}{3}\alpha_\varepsilon\varepsilon^{2/3}k^{-5/3}$$

where k is the wave number in radians per meter, $S_{ww}(k)$ is the power spectral density of the vertical velocity at k, and α_ε is the Kolmogorov constant, taken here to be 0.52.
23. J. B. Edson, C. W. Fairall, P. G. Mestayer, S. E. Larsen, *J. Geophys. Res.* **96**, 10689 (1991).
24. N. E. Busch and H. A. Panofsky, *Q. J. R. Meteorol. Soc.* **94**, 132 (1968). In our notation, their expression for the nondimensional vertical wind spectrum in the surface layer is

$$\frac{kS_{ww}(k)}{u_{*o}^2} = \frac{A(\omega/\omega_m)}{1 + 1.5(\omega/\omega_m)^{5/3}}$$

with $\omega = kz/(2\pi)$. They did not find similar simple expressions for the downstream or horizontal cross-stream spectra. They estimated the constants to be $A = 1.075$ and $\omega_m = 0.32$, where the latter is the nondimensional wave number at the peak in the spectrum and implies a value of 0.8 for $c_\lambda = \lambda_{peak}k_{max}$. Using our data from 4 m, assuming that surface-layer scaling held approximately at that depth, we found a better fit to the mean spectrum with a slightly higher value for ω_m, from which $c_\lambda = 0.85$.
25. M. G. McPhee and J. D. Smith, *J. Phys. Oceanogr.* **6**, 696 (1976).
26. Differentiation with respect to z of the steady Ekman (*20*) momentum equation with the substitution $\hat{\tau} = K\partial\hat{U}/\partial z$, yields $(if_{cor}/K)\hat{\tau} = d^2\hat{\tau}/dz^2$, with solution $\hat{\tau} = \hat{\tau}_o e^{a(1-i)z}$ (southern hemisphere) where $a = \sqrt{|f_{cor}|/(2K)}$.
27. M. G. McPhee, *J. Phys. Oceanogr.* **9**, 388 (1979).
28. This research was funded by the Office of Polar Programs, National Science Foundation (grants OPP9110422 and OPP9025083) and by the Office of Naval Research (contract N00014-84-C-0028). We thank R. Andersen and T. Baker for excellent field support and V. Lukin and J. Ardai for scientific and logistic support. The CTD data were kindly supplied by A. Gordon and B. Huber. Lamont-Doherty Earth Observatory contribution 5143.

23 August 1993; accepted 5 November 1993

Root-Knot Nematode–Directed Expression of a Plant Root–Specific Gene

Charles H. Opperman, Christopher G. Taylor, Mark A. Conkling*

Root-knot nematodes are obligate plant parasites that induce development of an elaborate feeding site during root infection. Feeding-site formation results from a complex interaction between the pathogen and the host plant in which the nematode alters patterns of plant gene expression within the cells destined to become the feeding site. Expression of *TobRB7*, a gene expressed only in tobacco roots, is induced during feeding site development. The cis-acting sequences that mediate induction by the nematode are separate from those that control normal root-specific expression. Reporter transgenes driven by the nematode-responsive promoter sequences exhibit expression exclusively in the developing feeding site.

Plant parasitic nematodes are among the most devastating pathogens of the world's food crops, causing an estimated $77 billion in food and fiber crop losses in 1987. The majority of this loss is caused by the root-knot nematodes (*Meloidogyne* spp.) (*1*). Root-knot nematodes are obligate sedentary endoparasites with a complex and intimate relationship with their host plants. The nematodes have a host range exceeding 2000 plant species (*2*). The primary symptom of root-knot nematode infection is the formation of enlarged galls on roots of susceptible host plants. Nutrient and water uptake are substantially reduced because of the damaged root system, resulting in weak and poor-yielding plants.

Nematode growth and reproduction depend on establishment of modified feeding sites within the plant root. The infective second-stage juvenile nematode (J2) moves freely through the soil. The J2 penetrates the root intercellularly in the region just posterior

C. H. Opperman, Department of Plant Pathology, North Carolina State University, Raleigh, NC 27695–7616.
C. G. Taylor and M. A. Conkling, Department of Genetics, North Carolina State University, Raleigh, NC 27695–7614.
*To whom correspondence should be addressed.

to the root cap and migrates to the developing vascular cylinder. The nematode then injects esophageal-gland secretions into the protophloem cells surrounding its head, resulting in the development of specialized multinucleate feeding cells called giant cells (*3*). The giant cells, acting as nutrient sinks (*4*), function as a permanent feeding site for the nematode (*5*). The five to seven giant cells associated with each developing nematode undergo rapid nuclear divisions without cytokinesis, resulting in multiple enlarged lobed nuclei. Increased numbers of cell organelles and protoplastids are observed, and the cells are metabolically highly active (*6*). A characteristic feature of giant cells is the elaborate network of membranous cell wall ingrowths, typical of transfer cells (*7*). These cell wall ingrowths increase surface area of the associated membrane and facilitate the import of elaborated photosynthates, minerals, and other metabolites on which the nematode feeds. During establishment of the giant cells, the nematode loses the ability to move and enlarges from the normal eel-shaped J2 to become a pear-shaped adult female. As the nematode feeds, reproduction results in the deposition of 300 to 1000 eggs.

The genetic mechanisms controlling formation of the nematode feeding site are poorly understood. Many plant genes in both resistant and susceptible hosts are believed to be either induced or altered in their expression during nematode infection (*7–9*). For example, the expression of genes encoding structural proteins or constitutive enzymes may be enhanced to accommodate the increased cellular metabolism occurring during nematode infection. No genes encoding proteins with known functions have been isolated or characterized. One gene expressed in response to parasitism by the potato cyst nematode, *Globodera rostochiensis*, has been isolated from potato, but its role in feeding site formation remains unknown (*10*). Here we report the effects of root-knot nematode infection on expression of a root-specific gene product of known function and on the identification of the cis-acting sequences responsive to nematode infection.

The tobacco root-specific gene, *TobRB7*, encodes a protein (pRB7) that is a member of a family of membrane proteins believed to function as membrane channels (*11*). A number of these proteins have been shown to function as water channels when expressed in *Xenopus* oocytes (*12*). The protein pRB7 can function as a water channel but does not transport ions, sugars, or charged amino acids (*13*). In situ hybridization to root sections revealed that the gene is expressed at high levels in root meristematic and immature vascular cylinder regions (*14*). To define the cis-acting sequences responsible for root-specific expression of *TobRB7*, we constructed fusion genes with various 5′ flanking regions and β-glucuronidase (GUS) (*15*). Cis-acting sequences necessary for root-specific expression of the reporter reside within its 5′ flanking region, between 299 and 636 nucleotides 5′ of the site of transcription initiation (*14*). The tissue-specific profile of the GUS reporter gene expression correlates with those observed by in situ hybridizations, implying that GUS activity profiles are accurate reporters of *TobRB7* gene expression.

Root-knot nematodes are thought to affect expression of numerous plant genes. The properties of pRB7 correlate with functions expected in giant cells. To determine whether *TobRB7* is expressed in giant cells, we inoculated transgenic tobacco plants carrying *TobRB7*-reporter constructs (*14*) with species of *Meloidogyne* (Table 1). The infected roots were examined for GUS activity and nematode development beginning 24 hours after inoculation and continuing to 40 days postinoculation. By 4 days postinoculation, significant GUS activity in and around the nematode feeding site was observed (Fig. 1). The root continues to grow after infection such that a feeding site initiated in immature root tissues is found later in the fully developed vascular system, a region in which *TobRB7* is not normally expressed (*14*). Root-knot nematode–infected roots

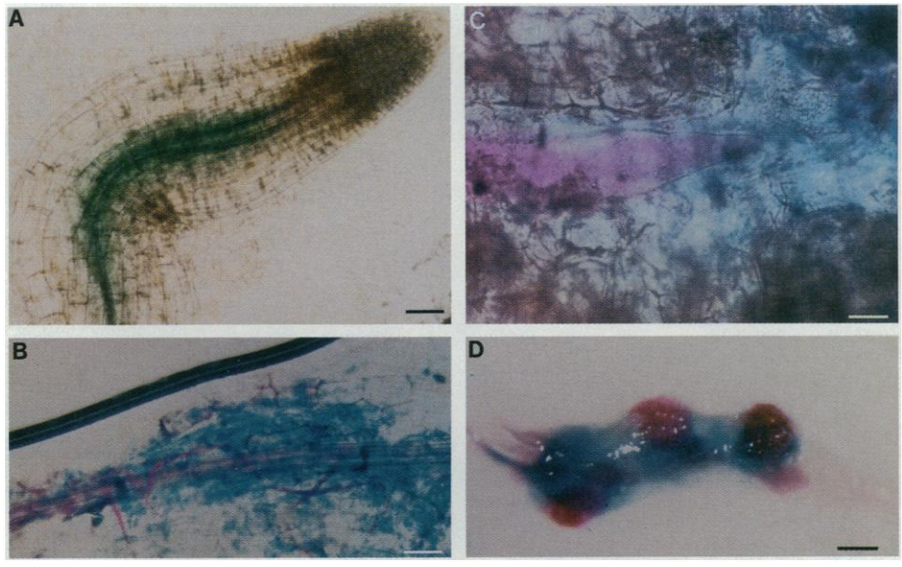

Fig. 1. Alteration of *TobRB7* expression patterns by root-knot nematode (*Meloidogyne incognita*) infection. (**A**) Normal expression of *TobRB7* in an uninfected root. Adapted from (*14*) with permission from the American Society of Plant Physiologists. (**B** through **D**) Tobacco tissue after infection with root-knot nematodes. Transgenic tobacco was infected with freshly hatched (<24 hours old) infective juveniles. For experiments on agar plates, approximately 1000 surface-sterilized J2 per plant were pipetted along the roots. For experiments in soil, 5000 J2 per plant were used in a sterile 2:1 sand:soil mixture. Nematodes within roots were stained red with acid fuchsin in glacial acetic acid:ethanol (1:1) and then destained in saturated chloral hydrate. GUS activity was visualized as a blue reaction by incubation in 5-bromo-4-chloro-3-indolyl-β-D-glucuronic acid (X-Gluc). We observed GUS activity around the parasitizing nematodes as early as 4 days after inoculation (B). (C) Optical section with a developing root-knot nematode J2 within the root 12 days after inoculation. By this point in the infection cycle, GUS is not detected in uninfected portions of the root vascular tissue at similar anatomical locations. (D) Three adult female nematodes 35 days after inoculation. The characteristic root gall has formed by cortical cell hyperplasia, and the swollen female nematodes have ruptured through the root surface to begin egg deposition. The root tissue surrounding the nematode infection has fully matured, yet GUS activity has continued in and around the feeding sites. Scale bars: (A), 8 μm; (B), 80 μm; (C), 20 μm; (D), 1.4 mm.

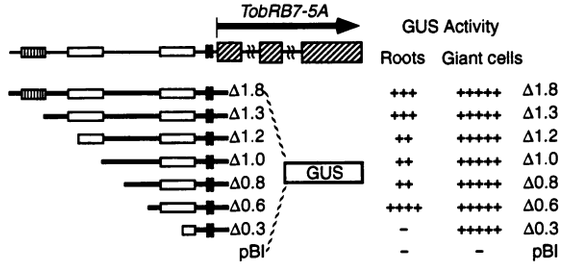

Fig. 2. Expression analysis of the *TobRB7* 5′ deletion series fused to GUS. The structure of the gene and the repeats in the promoter region have been described (*14*). Expression in infected and uninfected plants is summarized. Expression in leaves or other tissues has never been observed.

exhibit significantly different GUS activity patterns than do uninfected roots, the most striking of which is a temporal shift in GUS staining patterns. Normally, GUS expression is limited to cells in the elongation region of the roots. During nematode infection and development, GUS accumulates continuously in the giant cells over the entire 40-day period, even though they become surrounded by mature differentiated vascular tissue.

The cis-acting sequences necessary for root-specific expression are located between 299 and 636 bases 5′ of the initiation of transcription. No expression of the GUS reporter gene was observed in deletions containing only 299 bases of 5′ flanking sequence (Δ0.3) (*14*). To delineate the *TobRB7* cis-acting sequences responding to nematode infection, we inoculated numerous independent transgenic plants carrying the various 5′ deletions of the *TobRB7* 5′ flanking region fused to GUS. *Meloidogyne arenaria* infection resulted in GUS expression in giant cells of all *TobRB7* transgenic plants, including those with the Δ0.3 constructs (Fig. 2). No GUS expression was observed in transgenic plants (pBI) carrying the promoterless GUS gene from the *Agrobacterium*-binary plasmid vector pBI 101 (*15*). In the Δ0.3 constructs, GUS activity appeared to be limited to the giant cells (Fig. 3 and Table 1). A similar expression pattern is seen in transgenic potato carrying the Δ0.3 construct (*16*).

Table 1. Induction of Δ0.3 *TobRB7-GUS* by root-knot nematodes.

Nematode species host race*	Induction	Independent transformants (*n*)
Meloidogyne arenaria		
Race 1	Yes	>25
Meloidogyne incognita		
Race 1	Yes	>25
Race 2	NT†	0
Race 3	Yes	5
Race 4	Yes	>25
Meloidogyne javanica	Yes	5
Globodera tabacum	No	5

*Nematode host races were determined by host preference tests (*2*) and species identities confirmed by isozyme analysis. †NT, not tested.

Expression of the *TobRB7-GUS* transgene is not induced by high NaCl concentrations (up to 0.4 M), plant hormones (cytokinins and auxins), or wounding (*17*). The tobacco cyst nematode, *Globodera tabacum*, which also induces specialized feeding sites, does not induce expression of *TobRB7-GUS* (Table 1). The feeding sites of root-knot and cyst nematodes have some morphological similarities but are thought to be induced by a different mechanism (*7*). Our results support the concept that the feeding sites of cyst nematodes are distinct from those of *Meloidogyne*.

Cis-acting sequences regulating eukaryotic gene expression are frequently combinatorial (*18*). In evolving molecular mechanisms to establish feeding sites, the root-knot nematode has recruited plant genes to be expressed in specific spatial, developmental, and temporal patterns and, in the case of *TobRB7*, has circumvented the requirement for cis-acting sequences located between nucleotides 636 and 299 5′ of the initiation of transcription. It remains unclear whether this involves direct interaction of the nematode's glandular secretions with the *TobRB7* promoter or (as we believe more likely) indirect interactions in the developmental cascade. In any case, the normal pattern of *TobRB7* gene expression has been uncoupled from pathogen-induced gene expression. The function of pRB7 at feeding sites is unknown, although it may help maintain osmotic regulation.

The truncated *TobRB7* promoter has great potential in the design of genetically engineered crop plants with generalized resistance to root-knot nematodes. Directed expression of foreign genes precisely in specialized cells induced by the root-knot nematode infection (giant cells in the developing vascular cylinder) may overcome many disadvantages of previously described pest-control strategies (*2*).

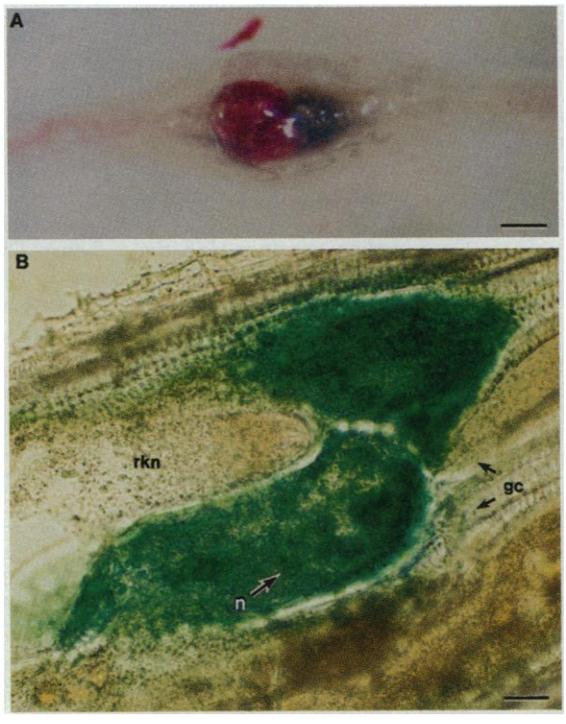

Fig. 3. Root-knot nematode–induced expression of GUS in the giant cells controlled by the Δ0.3 *TobRB7* promoter. GUS activity in plants carrying the Δ0.3 promoter was detectable only at the nematode feeding site. (**A**) Adult *M. arenaria* female in a root 35 days after inoculation. GUS activity was restricted to the central area of the infection site. (**B**) Section (40 μm) of developing *M. incognita* giant cells (12 days postinoculation) in a Δ0.3 *TobRB7-GUS* transformed plant. The nematode (rkn) has its head surrounded by two multinucleate (n) giant cells (gc). GUS activity is observed only in the giant cells. Scale bars: (A), 1.2 mm; (B), 20 μm.

REFERENCES AND NOTES

1. J. N. Sasser and D. W. Freckman, in *Vistas on Nematology*, J. Veech and D. Dickson, Eds. (Allen, Lawrence, KA, 1987), pp. 7–14.
2. J. N. Sasser, *Plant Dis.* **64**, 36 (1980).
3. R. S. Hussey, *Annu. Rev. Phytopathol.* **27**, 123 (1989).
4. A. F. Bird and B. R. Loveys, *J. Nematol.* **7**, 111 (1975); M. A. McClure, *ibid.* **9**, 88 (1977).
5. R. S. Hussey, in *An Advanced Treatise on* Meloidogyne, J. Sasser and C. Carter, Eds. (North Carolina State University Graphics, Raleigh, NC, 1985), vol. 1, pp. 143–153.
6. C. S. Huang, in (*5*), pp. 155–164.
7. M. G. K. Jones, *Ann. Appl. Biol.* **97**, 353 (1981).
8. P. Burrows, *J. Nematol.* **24**, 338 (1992).
9. D. J. Bowles, S. J. Gurr, C. Scollan, H. J. Atkinson, K. E. Hammond-Kosack, in *Biochemistry and Molecular Biology of Plant-Pathogen Interactions*, C. Smith, Ed. (Oxford Science, Oxford, 1991), pp. 225–236.
10. S. J. Gurr, M. J. McPherson, C. Scollan, H. J. Atkinson, D. J. Bowles, *Mol. Gen. Genet.* **226**, 361 (1991).
11. Y. T. Yamamoto, C.-L. Cheng, M. A. Conkling, *Nucleic Acids Res.* **18**, 7449 (1990).
12. G. M. Preston, T. P. Carroll, W. B. Guggino, P. Agre, *Science* **256**, 385 (1992); C. Maurel, J. Reizer, J. I. Schroeder, M. J. Chrispeels, *EMBO J.* **12**, 2241 (1993).
13. Y. Li, W. J. Lucas, M. A. Conkling, unpublished results.
14. Y. T. Yamamoto, C. G. Taylor, G. N. Acedo, C.-L. Cheng, M. A. Conkling, *Plant Cell* **3**, 371 (1991).
15. R. A. Jefferson, *Plant Mol. Biol. Rep.* **5**, 387 (1987).
16. C. P. Romano, C. H. Opperman, M. A. Conkling, unpublished results.
17. C. G. Taylor and M. A. Conkling, unpublished results.
18. T. Maniatis, S. Goodbourn, J. A. Fischer, *Science* **236**, 1237 (1987); P. N. Benfey, L. Ren, N.-H. Chua, *EMBO J.* **8**, 2195 (1989).

19. We thank G. N. Acedo and S. Chang for technical assistance; M. J. Hazouri for nutrient solutions; K. R. Barker, C.-I. Cheng, C. S. Levings III, P. B. Lindgren, and S. A. Lommel for critical reviews of the manuscript; and B. D. Kohorn and C. P. Romano for helpful discussions. Supported in part by the North Carolina Biotechnology Center, RJR Nabisco Inc., HybriTech Seed International Inc., NSF award MCB-9206506, and Department of Agriculture National Research Initiative award 92-37302-7640.

26 July 1993; accepted 13 October 1993